

# Hippocampal Sparing in Whole-Brain Radiotherapy: A Comparative Study of Helical Tomotherapy and Volumetric Modulated Arc Therapy

Palanivelu D<sup>1,2</sup>, D. Khanna<sup>1</sup>, P. Mohandass<sup>3</sup>, Vadiraja BM<sup>2</sup>, Sanjeev Sharma<sup>2</sup>, Sindhu P Kavalakkat<sup>2</sup>, Venugopal S<sup>1,4</sup>, Anto Vaz<sup>1,5</sup>

<sup>1</sup>Department of Physical Sciences, School of Sciences, Arts and Media, Karunya Institute of Technology and Sciences, Coimbatore, Tamil Nadu, India. <sup>2</sup>Department of Radiotherapy, Manipal Hospital, Old Airport Road, Bengaluru, Karnataka, India. <sup>3</sup>Department of Radiation Oncology, Fortis Cancer Institute, Fortis Hospital, Mohali, Punjab, India. <sup>4</sup>Department of Radiation Oncology, Yashoda Super Specialty Hospital and Cancer Institute, Ghaziabad, India. <sup>5</sup>Department of Radiation Oncology, Kovai Medical Center and Hospital, Coimbatore, India.

## Abstract

**Background:** Study to perform a dosimetric analysis and comparison of hippocampal (HC) sparing in whole-brain radiotherapy (WBRT) using volumetric modulated arc therapy (VMAT) and helical tomotherapy (HT). **Material and Methods:** Twenty patients who had previously undergone WBRT with a prescribed dose of 30 Gy in 10 fractions, incorporating HC sparing, were selected for this study. The HC was contoured, and HC avoidance (HCA) regions were defined using a 5.0 mm volumetric expansion around the HC. Treatment plans were created using Accuray Precision treatment planning for HT and Pinnacle treatment planning for Elekta Infinity with an Agility head using VMAT. For comparison, parameters including V100, V98, and V95 (volumes receiving 100%, 98%, and 95% of the prescribed dose, respectively), maximum dose (Dmax), mean dose (Dmean), conformity index (CI), and homogeneity index (HI) for the planning target volume (PTV) and PTV-HC were evaluated. Additionally, doses received by organs at risk (OAR), including the HC, eyes, and lenses, were analysed. **Results:** No significant differences in target coverage were observed between VMAT and HT for PTV and PTV-HC. V100 was comparable for both techniques (85% for PTV and 89% for PTV-HC), while V98 and V95 were slightly lower with VMAT for both targets. Dmax and Dmean values for PTV and PTV-HC were similar, and CI and HI were also comparable between the two techniques. VMAT provided improved sparing of OARs. The HC Dmax was reduced by 10.0% on the right and 11.7% on the left, while Dmean was reduced by 8.1% and 6.9%, respectively, compared to HT. VMAT significantly reduced eye doses, with Dmax reductions of 27.0% for the right eye and 22.4% for the left eye, and Dmean reductions of 15.5% and 18.0%, respectively. Lens Dmax was also lower with VMAT (right: 21.3%; left: 20.2%). VMAT significantly reduced beam-on time, with HT requiring approximately 64% longer treatment time. **Conclusion:** Target coverage was similar in both HT and VMAT plans, while VMAT achieved lower Dmax to the eyes and HC and reducing treatment time. Owing to improved OAR sparing and treatment efficiency, VMAT may be preferred for HCA-WBRT.

**Keywords:** Hippocampus- Helical Tomotherapy- VMAT

*Asian Pac J Cancer Biol*, 11 (2), 535-545

Submission Date: 02/17/2026 Acceptance Date: 04/05/2026

## Introduction

About 10% to 30% of adult cancer patients develop brain metastases (BM), which are the most common intracranial tumors in adults and a significant cause of

morbidity and mortality [1]. BM often indicate an advanced stage of disease and may pose a serious threat to the patient's life if treatment is delayed [2]. Whole-brain

## Corresponding Author:

Dr. D. Khanna

Department of Physical Sciences, School of Sciences, Arts and Media, Karunya Institute of Technology and Sciences, Coimbatore, Tamil Nadu, India.

Email: davidkhanna@karunya.edu

radiation therapy (WBRT) remains a key treatment option for most patients with BM, as it helps reduce the risk of death from neurological causes, improves intracranial disease control, and alleviates symptoms [3].

Preclinical and clinical studies suggest that radiation-induced cognitive impairment may be worsened by even low doses of radiation absorbed by neural stem cells in the sub granular zone of the hippocampal (HC) dentate gyrus [4]. Retrospective clinical studies and preliminary findings from prospective trials indicate that the HC plays a role in the early changes in cognitive function following radiation therapy [5]. Cognitive decline after radiation was previously considered a late side effect, attributed to neuroglial loss and microvascular damage. However, growing evidence points to both acute and subacute cognitive changes following radiation therapy, likely mediated through the HC and other neurogenic regions [6]. Although WBRT is a standard treatment for patients with BM, it is often associated with significant neurocognitive decline, primarily due to radiation-induced damage to the HC. HC sparing WBRT has emerged as an effective approach to reduce radiation-induced neurotoxicity while maintaining adequate tumor control. With advancements in image-guided techniques and treatment modalities such as intensity-modulated radiation therapy (IMRT) and volumetric modulated arc therapy (VMAT), it is now possible to spare the HC region without compromising target coverage.

This study addresses the absence of comprehensive dosimetric comparisons between helical Tomotherapy (HT) and VMAT platforms for HC avoidance (HCA) in WBRT. Although HT is known for its highly modulated intensity patterns due to binary Multileaf collimator (MLC) and fine slice-by-slice delivery, VMAT offers arc-based delivery with variable dose rates and gantry speeds. Despite these technical differences, there is a lack of studies evaluating which system provides superior Organ at sparing (OAR) sparing especially for the HC, eyes, and lenses while maintaining adequate target coverage.

To address these gaps, this study conducted a systematic dosimetric evaluation of HT and VMAT for HC sparing WBRT. Key parameters analyzed included volumes receiving 100%, 98%, and 95% of the prescribed dose (V100, V98, and V95) as well as maximum (Dmax) and mean (Dmean) doses to the PTV and PTV minus HC (PTV-HC), in addition to doses delivered to critical OARs. The findings aim to guide clinical decision making and optimize treatment planning, ultimately reducing neurocognitive side effects in patients undergoing WBRT. Aim of this study evaluates the dosimetric advantages of HC sparing in treatment planning using the Elekta Infinity with agility MLC, and HT with Radixact -X9 systems.

## Materials and Methods

A total of 20 patients who underwent WBRT between January 2024 and May 2025 were included in this study. Computed Tomography (CT) simulation was performed using a Philips Big Bore 16-slice CT scanner

(Philips Medical Systems, Cleveland, USA). Patients were positioned supine, with the head supported by an appropriate headrest and the arms placed alongside the body. CT images were acquired from the vertex to the fourth cervical vertebral (C4) level in a head-first, feet-down orientation, with a slice thickness of 3mm. The acquired images were transferred to the Varian Eclipse™ (Varian Medical Systems, Palo Alto, US) Treatment Planning System (TPS) for contouring. The target volume (whole brain) and OARs, including the HC and HCA regions (generated by applying a uniform 5-mm margin around the HC), were delineated. The eyes and lenses were also contoured with the aid of CT–Magnetic Resonance Imaging (MRI) image fusion, and all contours were reviewed and approved by an experienced radiation oncologist.

The CT images and corresponding structure sets were transferred to the Pinnacle® (Philips Medical Systems, Cleveland, USA) TPS for treatment planning. Upon import, auxiliary structures were generated to assist in the planning process. Treatment plans were created for an Elekta Infinity® (Stockholm, Sweden) linear accelerator (LINAC) equipped with an Agility MLC head, featuring 80 pairs of MLCs with a leaf width of 5 mm at the isocenter. VMAT plan was generated with the prescription dose of 3000cGy in 10 fractions using a 6 MV photon beam with three full arc rotations. Dose calculations were performed using the Adaptive Convolution algorithm, with the number of iterations set to 40. Plans were re-optimized iteratively until the desired dose coverage of the target volume and adequate sparing of OARs were achieved.

For comparison, a treatment plan was generated using the HT with Radixact X9® (Accuray, Madison, USA) system, which is equipped with 64 binary MLCs with a resolution of 6.25 mm at the isocenter. The Tomo Helical delivery mode with a dynamic jaw and a 2.5 cm field width was used for planning. Dose calculations were performed in the Accuray Precision® (Accuray, Madison, USA) TPS using the collapsed cone convolution algorithm. The dose distribution of HC sparing VMAT and HT plans in the axial, coronal, and sagittal views is shown in Figure 1.

## Results

Dosimetric evaluation of the PTV and PTV-HC was performed by analyzing the V100, V98, and V95, alongside the Dmax and Dmean. Treatment plan quality was further assessed using the conformity index (CI) and homogeneity index (HI) to evaluate the precision of dose conformity and uniformity within the target volumes as shown in Figure 2. In parallel, doses delivered to critical OARs, including the HC, eyes, and lenses, were carefully examined to ensure minimize the risk of radiation-induced toxicity. Comparison of OARs dose parameters between HT and VMAT as illustrated in Figure 3. This comprehensive assessment enabled an integrated evaluation of both target coverage and normal tissue sparing, providing a robust measure of overall plan quality and safety.

The mean HC volume was 2.21 cm<sup>3</sup> (range: 1.47–2.93 cm<sup>3</sup>). The mean volume of the HCA region was 27.51

Table 1. Comparison of Treatment Planning Parameters for PTV between VMAT and HT for V100, V98, V95, Dmax, Dmean, CI and HI.

S.NO	PTV													
	V100 (%)		V98 (%)		V95 (%)		Dmax (cGy)		Dmean (cGy)		CI		HI	
	VMAT	HT	VMAT	HT	VMAT	HT	VMAT	HT	VMAT	HT	VMAT	HT	VMAT	HT
1	86.1	85.2	88.9	91.9	91	93.6	3280	3230	3007	2993	0.86	0.85	1.3	1.2
2	85.1	84.8	87.9	91.6	91.5	94.4	3340	3319	3002	2982	0.85	0.85	1.4	1.1
3	85.4	85.2	88.6	92.3	90.8	94.5	3300	3330	2999.8	3008	0.85	0.85	1.4	1.1
4	85	84.8	88.1	93	90.3	94.4	3290	3256	2996.7	2987	0.85	0.85	1.3	1.1
5	86.2	86.8	90.3	92.3	93.2	93.9	3280	3251	3023.9	3021	0.86	0.87	1.1	1
6	84.1	83.7	87.1	88.8	90.6	91.6	3274	3313	2947	2945	0.84	0.84	1.4	1.5
7	83.1	84.8	88.3	89.8	91.2	92.3	3329	3407	2985.1	3001	0.83	0.85	1.3	1.2
8	83	84.2	87.1	91.2	89.6	93.1	3319	3270	2961.1	2998	0.83	0.84	1.6	1.1
9	86.2	85.6	88.6	90.6	91.4	93.1	3421	3244	2951	2992	0.86	0.86	1.5	1.2
10	83.5	84.7	86.5	92.8	89.8	94.4	3323	3268	3004	2997	0.84	0.85	1.4	1.1
11	86.2	86.8	87.6	92.4	90.1	94.2	3330.1	3330	2998	2998	0.86	0.87	1.2	1.1
12	85.6	83.9	87.1	93.2	90.6	95.1	3298	3289	3006	2992	0.86	0.84	1.2	1.1
13	83.1	85.3	89.4	91.6	91.7	92.8	3290	3390	2989	3018	0.83	0.85	1.4	1.1
14	84.2	86.1	88.1	89.8	90.8	93.1	3298	3296	2998.1	2977	0.84	0.86	1.4	1.1
15	85.2	83.6	89.8	91.8	91.1	91.8	3289	3331	3012.4	3011	0.85	0.84	1.5	1
16	82.9	84.1	87.7	89.9	89.9	92.5	3283	3293	2989	2995	0.83	0.84	1.6	1.1
17	86.1	85.2	88.1	89.8	90.3	93.2	3289	3307	2988	3011	0.86	0.85	1.3	1.2
18	86.5	84.6	88.3	92.3	91.1	91.5	3308	3327	2975	2989	0.87	0.85	1.2	1.1
19	86.3	85.1	89.3	91.1	91.4	92.3	3321	3344	2972	2997	0.86	0.85	1.3	1.2
20	85.9	84.9	87.6	90.6	89.8	94.2	3304	3298	2999	2992	0.86	0.85	1.3	1.1
Mean±SD	85±1.3	85.0±0.9	88.2±0.98	91.3±1.2	90.8±0.84	93.3±1.1	3308.3±32.6	3305±45.7	2990.2±20.1	2995.2±16.3	0.85±0.01	0.85±0.01	1.3±0.1	1.1±0.1
P Values	P=0.96		P<0.01		P<0.01		P=0.77		P=0.39		P=0.96		P<0.01	

cm<sup>3</sup> (range: 13.31–36.50 cm<sup>3</sup>). The average Whole Brain (WB) volume was 1481.07 cm<sup>3</sup> (range: 1093.70–1705.67 cm<sup>3</sup>), while the mean volume of the WB excluding the HCA region was 1453.55 cm<sup>3</sup> (range: 1057.20–1453.50 cm<sup>3</sup>). Overall, the HC constituted approximately 0.3% (range: 0.2–0.5%) of the total brain volume, whereas the HCA region accounted for 1.9% (range: 0.8–3.3%) of the brain volume.

No significant dose differences were observed between

the VMAT and HT plans in terms of PTV coverage. V100 was identical for both techniques (85% vs. 85%). V98 was slightly lower in the VMAT plan compared to the HT plan (88.2% vs. 91.3%), and a similar trend was noted for the V95 (90.8% vs. 93.3%). No notable differences were observed between VMAT and HT plans in the Dmax (3308.3 cGy vs. 3305 cGy) and Dmean (2990 cGy vs. 2995.2 cGy). Likewise, CI and HI were comparable between the two techniques (CI: 0.85 vs. 0.85; HI: 1.3 vs.

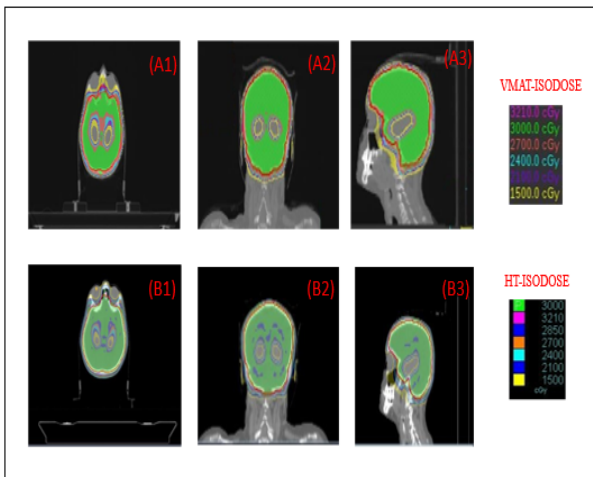


Figure 1. Dose distribution of HC-sparing for the VMAT plan in (A1) axial, (A2) coronal, and (A3) sagittal views, and for the HT plan in (B1) axial, (B2) coronal, and (B3) sagittal views

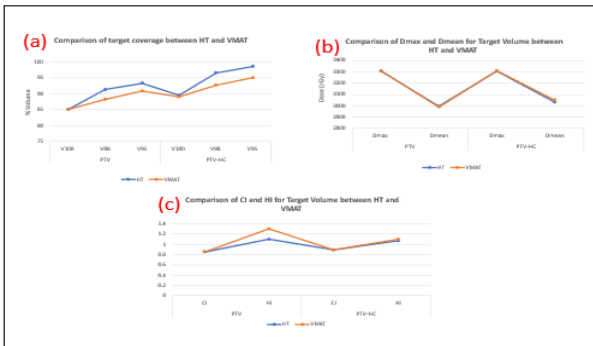


Figure 2. Treatment planning parameters comparing HT and VMAT for the target volume: (a) PTV and PTV-HC coverage, (b) Dmax and Dmean for PTV and PTV-HC, and (c) CI and HI for PTV and PTV-HC

1.1) as shown in Table 1.

For planning purposes, the PTV-HC structure was generated by subtracting the HC from the PTV. This derived volume represents the portion of the brain requiring full prescription dose coverage while excluding the HCA region. Dose prescription and optimization constraints were applied specifically to the PTV-HC to ensure adequate target coverage and conformity, while maintaining dose limitations to the HC to minimize the risk of neurocognitive impairment. No significant dose differences were observed between the VMAT and HT plans in terms of PTV-HC coverage. The volume of PTV-HC of V100 was comparable between VMAT and HT (89.0% vs. 89.5%). V98 was slightly lower in VMAT compared to HT (92.7% vs. 96.5%), and a similar trend was observed for the V95 (95.0% vs. 98.6%). No notable differences were found in the Dmax (3308.6 cGy vs. 3304.7 cGy) and Dmean (3050 cGy vs. 3032.3 cGy) between the two plans. Likewise, the CI and HI were nearly identical for VMAT and HT (CI: 0.89 vs. 0.89; HI: 1.10 vs. 1.07) as illustrated in Table 2.

The Dmax to the HC was lower in the VMAT plan compared to the HT plan. For the right HC, the Dmax was 1153.3 cGy with VMAT and 1281.9 cGy with HT, while for the left HC it was 1121.1 cGy and 1269.2 cGy,

respectively. The Dmean to the right (1018.8 cGy vs. 1101.8 cGy) and left (995.1 cGy vs. 1069.1 cGy) HC were nearly equivalent between the two techniques as indicated in Table 3.

The Dmax to the right eye was significantly lower in the VMAT plan compared to the HT plan (1420.0 cGy vs. 1839.1 cGy), as was the dose to the left eye (1392.1 cGy vs. 1794.1 cGy). Similarly, the Dmean to the right eye (853.8 cGy vs. 1011.0 cGy) and left eye (825.9 cGy vs. 1008.1 cGy) was slightly lower with VMAT as shown by Table 4. The Dmax to the right lens (723.7 cGy vs. 920.5 cGy) and left lens (715.9 cGy vs. 897.7 cGy) were also lower in the VMAT plan compared to the HT plan. However, no notable differences were observed in the Dmean for lenses, which were 612.9 cGy vs. 593.9 cGy for the right lens and 607.6 cGy vs. 659.4 cGy for the left lens as reflected in Table 5. Additionally, we compared the beam on time of HT and VMAT plan. The results of this study indicate that the treatment beam-on time was significantly longer for HT (508.1 seconds) compared to VMAT (182.6 seconds) as illustrated in Table 5.

Statistical analyses were performed using a paired t-test in SPSS Statistics (version 31.0) to compare Dose Volume histogram (DVH) metrics and OAR doses between VMAT and HT plans. A p-value of < 0.05 was considered statistically significant.

## Discussion

The HC, a critical component of the limbic system, plays a pivotal role in learning, memory, emotion, motor control, endocrine regulation, and short-term memory storage. It is located in the medial temporal lobe of the brain, with one HC present on each hemisphere [7, 8]. The medial portion of the temporal lobe contains the characteristic S-shaped structure of the HC. Neurogenesis has been shown to occur within the HC [9], which is fundamental for cognition, memory formation, and spatial navigation [10]. According to Le Fèvre et al. [11], an increase of 100cGy in the equivalent dose of 200cGy (EQD2) delivered to the left HC may elevate the risk of neurocognitive deterioration, particularly in verbal memory recall, by up to fourfold.

Anatomically, the HC consists of two U-shaped interconnecting laminae: the dentate gyrus and the cornu ammonis. It forms an integral part of the limbic circuit, encompassing gray matter structures such as the parahippocampal gyrus and amygdala, and white matter tracts including the fimbriae and fornices, which constitute the primary efferent pathways of the HC. The pyramidal and granule cells located within the dentate gyrus are strongly associated with memory processing and consolidation [12]. Preclinical evidence indicates that the neural stem cell compartment of the dentate gyrus is essential for HC neurogenesis [13, 14]. Damage to this region following cranial irradiation significantly accelerates neurocognitive decline, particularly in domains associated with memory function [15, 16].

According to previous research, HC tissue is highly radiosensitive, and even low radiation doses can result

Table 2. Comparison of Treatment Planning Parameters for PTV-HC between VMAT and HT for V100, V98, V95, Dmax, Dmean, CI and HI.

S.NO	PTV-HC													
	V100 (%)		V98 (%)		V95 (%)		Dmax (cGy)		Dmean (cGy)		CI		HI	
	VMAT	HT	VMAT	HT	VMAT	HT	VMAT	HT	VMAT	HT	VMAT	HT	VMAT	HT
1	90.6	91	93.2	96.8	95.8	98.5	3281	3230	3078	3054	0.91	0.91	1.1	1
2	89	88.9	92.4	95.8	95.7	98.6	3340	3320	3067	3031	0.89	0.89	1.1	1.1
3	89.1	89.4	92.5	96.7	94.8	98.3	3300	3330	3067	3029	0.89	0.89	1.1	1
4	89.5	89.6	93	98.1	95.4	99.4	3290	3256	3070	3038	0.9	0.9	1.1	1
5	90.4	91.1	93.2	96.4	96	98.6	3280	3250	3057.1	3043	0.9	0.91	1.1	1
6	87.1	88.3	92.3	96.5	94.8	98.6	3274	3313	3050	2970	0.87	0.88	1.1	1.2
7	88.6	89.2	92.8	96.7	96.7	97.8	3329.5	3405	3057	3058	0.89	0.89	1.1	1.2
8	86.9	88.8	91.3	95.7	90.7	98.6	3319.2	3270	3014.2	3038	0.87	0.89	1.2	1.1
9	87.3	89.6	91.6	97	94.8	99.1	3421.6	3244	3048.4	3055	0.87	0.9	1.1	1.1
10	87.2	88.5	90.2	96.9	95.7	98.5	3323	3268	3069	3038	0.87	0.89	1.3	1.1
11	89.3	89.6	94.1	96.2	94.8	98.5	3331	3330	3088	3044	0.89	0.9	1.1	1
12	88.9	88.5	91.2	97.1	96.7	98.8	3297	3290	3057	3035	0.89	0.89	1.1	1.1
13	89.8	89.8	92.8	96.2	93.8	97.9	3290	3390	3045	3025	0.9	0.9	1.1	1
14	89.8	89.6	94.7	96.5	94.4	99.2	3298	3298	3032	3036	0.9	0.9	1.1	1
15	87.6	88.4	93.9	97.1	95.4	98.3	3289	3331	3036	3023	0.88	0.88	1.1	1
16	90.2	89.8	93.5	96.1	93.8	98.9	3285	3293	3043	3010	0.9	0.9	1.1	1.1
17	89.3	90.1	93.9	95.7	96.7	98.1	3288	3308	3067	2998	0.89	0.9	1.1	1.1
18	87.8	89.6	92.1	96.4	94.9	98.9	3309	3327	3012	3027	0.88	0.9	1.1	1.1
19	90.2	89.9	92.5	97.1	93.8	99.3	3321	3344	3028.1	3046	0.9	0.9	1.1	1
20	91.1	90.2	92.3	95.7	95.7	99.2	3306	3297	3013.8	3048	0.91	0.9	1.1	1.1
Mean±SD	89.0±1.3	89.5±0.8	92.7±1.1	96.5±0.6	95.0±1.4	98.6±0.5	3308.6±32.7	3304.7±45.5	3050±21.9	3032.3±20.8	0.89±0.01	0.89±0.01	1.1±0.05	1.07±0.05
P Values	P=0.13		P<0.01		P<0.01		P=0.75		P<0.01		P=0.13		P<0.01	

in damage to the HC region, leading to progressive and irreversible memory loss and dementia. Such effects can significantly diminish patients' quality of life (QOL) [17, 18]. Therefore, the radiation therapy team must pay particular attention to accurately contouring the HC, selecting optimal planning parameters and dose constraints, and determining appropriate dose metrics, setup, and delivery techniques to achieve effective HC

sparing. Given its central location within the brain, precise delineation of the HC is essential to minimize the risk of intracranial disease progression while maintaining the potential neurocognitive benefits of HC preservation. generating an optimized WB irradiation plan that adequately spares the HC remains challenging due to its complex anatomical shape and midline location. Nevertheless, HCA can be effectively achieved using

Table 3. Comparison of OAR doses between VMAT and HT Plans for Left and Right HC

S.NO	LEFT HC				RIGHT HC			
	Dmax (cGy)		Dmean (cGy)		Dmax (cGy)		Dmean (cGy)	
	VMAT	HT	VMAT	HT	VMAT	HT	VMAT	HT
1	1140	1213	1083	998	1185	1245	1129	995
2	1090	1260	1003	1034	1170	1330	1006	1064
3	1040	1285	956.3	1109	1055	1262	945.1	1118
4	1140	1273	1066.5	1105	1150	1268	1095.4	1170
5	1080	1213	915.2	1065	1070	1332	992.5	1168
6	1085	1180	1036.8	990	1107	1227	1024.1	1005
7	1220	1301	980.3	1050	1242	1286	980.6	1051
8	1221	1235	982.2	1058	1197.6	1270	987.4	1043
9	1069	1310	961.5	1157	1114.1	1281	1021.9	1168
10	1190	1289	1007	1187	1190	1315	1025.8	1174
11	1080	1267	1002	1121	1172	1321	1123	1086
12	1165	1308	1011	1134	1182	1236	1014	1088
13	1122	1245	968	1087	1065	1286	958.6	1139
14	1153	1282	972	997	1127	1342	989.4	1087
15	1075	1248	937	1045	1088	1316	1026.8	1136
16	1065	1302	1027.1	1121	1210.3	1216	1013.8	1015
17	1232	1287	994.7	1032	1138.1	1208	1014.6	1065
18	1122	1294	988.3	995	1260.1	1347	978.9	1140
19	1101	1272	1012.7	990	1128.4	1290	1013.8	1157
20	1032	1321	998.3	1106	1215.3	1260	1035.6	1166
Mean± SD	1121.1±60.3	1269.2±37.2	995.1±40.1	1069.1±59.7	1153.3±59.0	1281.9±42.3	1018.8±48.2	1101.8±59.7
P Values	P<0.01		P<0.01		P<0.01		P<0.01	

advanced IMRT techniques, such as HT and VMAT, while maintaining sufficient target volume coverage and dose homogeneity [12].

In a Phase II clinical trial conducted in collaboration with the European Organization for Research and Treatment of Cancer (EORTC) and the Radiation Therapy Oncology Group (RTOG), researchers evaluated the feasibility of reducing the radiation dose to the HC region during WBRT. The primary HC dose constraint in this study was a Dmax of  $\leq 1600$  cGy, with permissible variations up to Dmax  $\leq 1700$  cGy, for a prescription dose of 3000 cGy delivered in 10 fractions [19]. Subsequently, a Phase III clinical trial by Dr. Paul D. Brown and colleagues [3] validated the benefits of employing IMRT to spare the HC neurogenic stem-cell niche during WBRT. Compared with standard WBRT, HCA-WBRT combined with memantine significantly preserved cognitive function and reduced patient-reported symptoms, without increasing toxicity or compromising intracranial progression-free survival or overall survival. Based on these findings, HCA-WBRT with concurrent memantine is recommended as the standard treatment approach for patients with BM who have a satisfactory performance status and are scheduled to undergo WBRT.

According to Kim et al. [20], HCA-WBRT with simultaneous integrated boost (SIB) for patients with 1–3 BMs, HyperArc produces better dosimetric plans compared with RapidArc. In their retrospective analysis of 19 patients, treatment plans prescribed 2500 cGy to the brain PTV and 4500 cGy to the metastatic PTV delivered

in ten fractions. HyperArc demonstrated improved target conformity and coverage, along with enhanced HC sparing. Notably, the Dmax to the HC was significantly lower with HyperArc than with RapidArc (1553 cGy vs. 1671 cGy). Furthermore, HyperArc provided better protection of the HC and other OARs across both delivery modes. Their findings suggest that HyperArc is a promising alternative for HCA-WBRT with SIB, as it achieves superior plan quality, improves target metrics, and reduces HC dose, thereby potentially preserving neurocognitive function while effectively treating BMs. Corrao et al. [21] evaluated plan quality for HCA-WBRT with SIB in patients with BMs using different techniques: HyperArc, VMAT, and HT. Their findings showed that

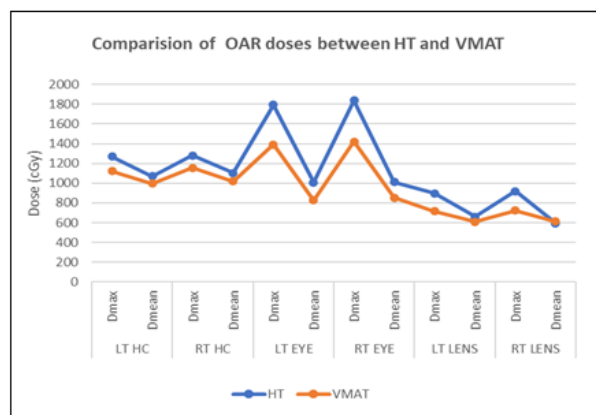


Figure 3. Comparison of OAR Dose Parameters between HT and VMAT

Table 4. Comparison of OAR Doses between VMAT and HT Plans for Left and Right Eye

S.NO	LEFT EYE				RIGHT EYE			
	Dmax (cGy)		Dmean (cGy)		Dmax (cGy)		Dmean (cGy)	
	VMAT	HT	VMAT	HT	VMAT	HT	VMAT	HT
1	1580	1847	880.4	921	1430	1944	980.4	1091
2	1400	1755	784.4	998	1380	1915	806.1	1064
3	1520	1966	763.5	1021	1540	1820	779.3	995
4	1420	1855	894	1020	1480	1861	873.9	1053
5	1460	1678	1004.8	1108	1520	1787	880.3	1142
6	1306	1860	761.2	989	1406	1784	786.8	987
7	1234.9	1954	775.2	987	1354.8	1707	748.9	993
8	1345.6	1623	780.6	1020	1280.1	1845	703.6	1043
9	1332.8	1819	994.2	987	1256.2	1926	994	929
10	1366	1609	755	1030	1351	1846	748	912
11	1486	1717	788.3	921	1530	1874	883.7	1023
12	1423	1885	923.4	998	1488	1725	876.3	1012
13	1528	1761	883.9	1021	1345	1837	889.4	1026
14	1220	1832	902	1020	1390	1912	837.8	983
15	1480	1728	723.4	1108	1540	1887	780.5	889
16	1428	1960	812	989	1428	1823	886.1	998
17	1334.8	1781	770.8	987	1456	1723	848.8	1010
18	1289.7	1623	783	1020	1420.1	1880	904.8	1021
19	1420.6	1799	761.8	987	1354.7	1748	990.1	1036
20	1266	1829	776	1030	1458	1938	878.1	1012
Mean± SD	1392.1±100.8	1794.1±108.7	825.9±82.6	1008.1±45.7	1420.4±82.7	1839.1±73.9	853.8±81.1	1011±57.9
P Values	P<0.01		P<0.01		P<0.01		P<0.01	

VMAT achieved the lowest doses to several OARs, HT provided the greatest HC sparing and superior boost coverage, while HyperArc yielded the best WB coverage.

Liu R. et al. [22] reviewed the clinical application of HCA-WBRT for BMs, highlighting key clinical challenges, technological advances in HC contouring and treatment delivery, and potential future strategies to mitigate radiation-induced cognitive decline. By sparing HC neural stem cells, HCA-WBRT has been shown to better preserve neurocognitive function compared with conventional WBRT. Nevertheless, ongoing debate persists due to inconsistent results across clinical trials and variability in recommended HC dose constraints, with reported limits ranging from Dmax < 900–1400 cGy and Dmean < 600–800 cGy.

One of the earliest studies to demonstrate the feasibility of LINAC based static IMRT for HCA-WBRT was conducted by Gondi et al. [12]. Treatment planning was performed using the Pinnacle<sup>3</sup> TPS, with optimization involving nine static non-coplanar beams and six defined planning structures, including the PTV, HC, eyes, and lenses. The study achieved satisfactory target coverage and dose homogeneity while effectively sparing the HC, with a reported HC Dmean of 730 cGy. according to Yokoyama et al. [23], HT provided better sparing of the HC, eyes, and lenses compared to Halcyon-based HCA-WBRT plans. however, it demonstrated slightly better target coverage and substantially longer treatment delivery times. In contrast, a study by Jiang et al. [24]

reported no significant differences in the mean HC dose among HT, IMRT, and VMAT plans. Andreas et al. [25] further enhanced the efficiency of HCA-WBRT delivery in the RTOG-0933 trial by treating 14 patients using only seven coplanar beams. Eleven of the treatment plans met all protocol-specified dose constraints, while three were within the acceptable variation limits for the HC. However, the authors noted several unfavourable dosimetric patterns associated with this beam arrangement, including hotspots anterior to the HC and elevated mean PTV doses.

In a study by Deepshikha G. et al. [26], HCA-WBRT using LINAC-based VMAT was shown to be a feasible treatment approach for patients with BMs treated at a regional cancer center in Eastern India. The technique was associated with preservation or improvement of neurocognitive function and quality of life (QOL). The study included 27 patients who received 3000 cGy in 10 fractions using VMAT on an Elekta Synergy LINAC with Monaco treatment planning. Bilateral HC were contoured according to the RTOG 0933 atlas, with a 5-mm HCA margin applied. Planning objectives ensured PTV V3000cGy ≥ 90% and D2% ≤ 4000 cGy. Neurocognitive function was assessed using the Hopkins Verbal Learning Test–Revised Delayed Recall (HVLT-R DR), and QOL was evaluated using the Functional Assessment of Cancer Therapy–Brain (FACT-Br) questionnaire at baseline and during follow-up periods ranging from 2 to 12 months. HCA-WBRT preserved memory recall, consistent with the findings of RTOG 0933, which reported a mean

Table 5. Comparison of OARs Doses for Left, Right Lens and Treatment Time between VMAT and HT Plans

S.NO	LEFT LENS				RIGHT LENS				TREATMENT TIME (sec)		
	Dmax (cGy)		Dmean (cGy)		Dmax (cGy)		Dmean (cGy)		VMAT	HT	
1	VMAT	HT	VMAT	HT	VMAT	HT	VMAT	HT	VMAT	HT	
2	775	962	732.3	712	720	785	833	648.4	678	179.5	573.1
3	680	883	623.1	621	785	1011	1011	632.4	612	201.5	520.9
4	730	872	638.8	652	750	860	860	680.4	583	199.5	476.3
5	790	956	707	612	780	880	880	725.6	544	178	517
6	680	837	626.8	705	720	941	941	674.2	658	111	543.4
7	701.5	987	615.3	742	659.3	980	980	553.5	530	202	541.9
8	655	872	531.3	618	616.1	806	806	516.1	658	217	486.7
9	691	856	516.6	621	696.5	924	924	550	518	159.9	478
10	770.8	956	626.6	632	702.5	812	812	599.5	606	187.5	486.1
11	670.4	766	585.2	737	670	947	947	585.9	621	198	469.7
12	718	965	628.5	712	716	943	943	638.2	635	189.5	543.5
13	718.1	878	610	687	688	989	989	639.6	624	191.5	510.2
14	780.7	888	598.5	664	713	885	885	670.1	543	189.6	576.1
15	663	986	654.3	612	718	891	891	635.6	580	178	527.2
16	620	885	580.3	725	812	1041	1041	688.1	628	171	536.2
17	715	887	620.1	518	745	1010	1010	616	543	193	521.1
18	689	998	550.1	528	787	890	890	528.3	558	177	456.1
19	726	887	509.7	728	788	859	859	565.9	618	148.7	468.2
20	773.9	756	610.1	723	695.3	932	932	534.9	621	197.5	467.1
Mean± SD	770.1	876	588.2	639	712.3	976	976	575.1	519	184	463.8
P Values	715.9±48.5	897.7±67.7	607.6±53.7	659.4±65.6	723.7±49.4	920.5±68.2	612.9±59.8	593.9±49.3	508.1±37.2	182.6±22.9	
	P<0.01		P<0.01		P<0.01		P<0.01		P=0.27		

decline of 7% compared with the historical decline of approximately 30%. These results support the concept of protecting neural stem cell function through HC sparing. Mean scores on the FACT-Br questionnaire showed a statistically significant improvement, particularly in the spiritual well-being (SWB) subscale, with an 8–12% increase observed at 2–6 months of follow-up. No grade ≥3 toxicities were reported, and preservation of neurocognitive function was associated with maintenance of QOL. Overall, HCA-WBRT delivered with VMAT appears to be a safe, dosimetrically feasible, and effective approach for neurocognitive preservation, with minimal risk of HC involvement.

In a study by Li Z. et al. [27], HCA-WBRT with SIB was shown to be a safe and effective treatment for lung cancer patients with BMs, particularly when metastatic lesions were located more than 1 cm from the HC. This prospective phase II study included 40 Chinese patients

treated with VMAT or HT, delivering 3000–3600 cGy in 18–20 fractions to the WB clinical target volume and 4400–5200 cGy to the gross tumor volume. The Dmean and Dmax HC doses achieved were 892 cGy and 1224 cGy, respectively. At six months, the Chinese version of the Hopkins Verbal Learning Test–Revised (HVLTR) immediate recall score showed a modest decline of 9.8%, supporting its applicability for neurocognitive assessment in Chinese patients. No grade ≥3 toxicities were observed; the most common adverse effects were grade 1–2 dizziness (25%) and nausea (27.5%).

Monje and colleagues [28] demonstrated that inflammation in the vicinity of neural stem cells within the brain plays a significant role in radiation-induced effects. Moreover, non-radiation stimuli, such as bacterial lipopolysaccharides, were found to produce comparable inflammatory responses. With the advent of modern IMRT techniques, including HT and LINAC-based IMRT,

it is now possible to conformally spare these neural progenitor cells during cranial irradiation, as they are anatomically clustered within the dentate gyrus of the HC [13]. By reducing the radiation dose delivered to the HC, it may be feasible to limit radiation-induced inflammation and mitigate alterations in the microenvironment of these anatomically localized neural stem cells.

This study showed that both HT and VMAT achieved satisfactory target coverage and effective HC sparing in WBRT. However, the VMAT plans generated on the Elekta Infinity® (Stockholm, Sweden) LINAC with the Agility head delivered lower maximum doses to the HC and eyes and lesser beam on time compared to the HT plans created on the Radixact system. A summary of target coverage, CI, and HI for PTV and PTV-HC comparing HT and VMAT is presented in Table 6. Similarly, Table 7 summarizes the OAR doses and treatment time for HT and VMAT.

These differences can be explained by various technical and dosimetric factors.

In VMAT, three 360° coplanar arcs were utilized, during which the beam continuously rotates while dynamically modulating the dose rate, gantry speed, and MLC leaf positions. The Elekta Infinity’s Agility head, featuring 160 leaves with a 5 mm width at isocenter, provides a high leaf speed of up to 6.5 cm/s, enabling faster beam-on times and low interleaf transmission (<0.5%) [29]. These characteristics allow precise modulation around small and concave avoidance structures such as the HC and eyes. The combination of continuous gantry rotation and variable dose rate enhances intensity optimization, producing steeper dose gradients around OARs. HT, on the other hand, employs a helical fan-beam delivery technique in which the couch moves continuously as the gantry rotates. This continuous movement, along with other planning parameters such as pitch, modulation factor, and beam width, contributes to longer treatment times in HT. The system utilizes a binary MLC with 64 leaves that are either fully open or fully closed, limiting its modulation complexity compared to the analog MLCs used in VMAT systems. Although HT provides excellent longitudinal dose uniformity, its lateral modulation resolution is relatively coarse [30], making it slightly less effective in sparing small lateral OARs.

In HT, the use of a fixed fan-beam width can lead to low-dose spillover into anterior and lateral regions. In contrast, VMAT utilizes dynamically shaped fields that can be constrained to minimize unnecessary entrance doses through anterior structures. Furthermore, the backup jaw in VMAT helps reduce leakage and scatter to OARs located superior and inferior to the PTV, benefiting sensitive structures such as the HC and eyes situated near the brain midline and anterior skull base. VMAT also allows optimization of collimator angles to distribute MLC leaf leakage and limit direct irradiation to nearby OARs. In this study, collimator angles of 20° and 340° were selected. Conversely, HT operates with a fixed collimator angle of 0°, restricting the planner’s ability to control the direction of leakage and scatter distribution, which may result in slightly higher low-dose exposure to adjacent OARs.

Table 7. Summary of OARs Doses and Treatment Time Comparing HT and VMAT Plans.

Treatment Plan	LT HC		RT HC		LT EYE		RT EYE		LT LENS		RT LENS		Treatment Time (sec)
	Dmax (cGy)	Dmean (cGy)	Dmax (cGy)	Dmean (cGy)	Dmax (cGy)	Dmean (cGy)	Dmax (cGy)	Dmean (cGy)	Dmax (cGy)	Dmean (cGy)	Dmax (cGy)	Dmean (cGy)	
HT	1269.2±37.2	1069.1±59.7	1281.9±42.3	1101.8±59.7	1794.1±108.7	1008.1±45.7	1839.1±73.9	1011±57.9	897.7±67.7	659.4±65.6	920.5±68.2	593.9±49.3	508.1±37.2
VMAT	1121.1±60.3	995.1±40.1	1153.3±59.0	1018.8±48.2	1392.1±100.8	825.9±82.6	1420.4±82.7	853.8±81.1	715.9±48.5	607.6±55.7	723.7±49.4	612.9±59.8	182.6±22.9

Table 6. Summary of Target Coverage, CI, and HI Comparing HT and VMAT Plans for PTV and HC-PTV

Treatment Plan	PTV						HC-PTV							
	V100 (%)	V98 (%)	V95 (%)	Dmax (cGy)	Dmean (cGy)	CI	HI	V100 (%)	V98 (%)	V95 (%)	Dmax (cGy)	Dmean (cGy)	CI	HI
HT	85.0±0.9	91.3±1.2	93.3±1.1	3305±45.7	2995.2±16.3	0.85±0.01	1.1±0.1	89.5±0.8	96.5±0.6	98.6±0.5	3304.7±45.5	3032.3±20.8	0.89±0.01	1.07±0.05
VMAT	85±1.3	88.2±0.98	90.8±0.84	3308.3±32.6	2990.2±20.1	0.85±0.01	1.3±0.1	89.0±1.3	92.7±1.1	95.0±1.4	3308.6±32.7	3050±21.9	0.89±0.01	1.1±0.05

The HC shows substantial inter-patient variability in size, shape, and position, which can complicate accurate delineation. Anatomical differences, postoperative changes, edema, or tumor-related distortion increase uncertainty in HC contouring and dose delivery. Although anatomical changes during WBRT are usually limited, they may still affect the consistency of HC sparing. HCA-WBRT requires steep dose gradients around the HC, making plans sensitive to setup errors and contouring inaccuracies. Even small translational or rotational errors can increase HC dose or compromise target coverage. Variations in optimization methods and dose-calculation algorithms across planning systems may also influence plan robustness. Despite rigid immobilization, intra-fraction motion cannot be completely avoided. Longer treatment times with highly modulated techniques increase the risk of patient movement, which can blur dose gradients and reduce the effectiveness of HC sparing.

This dosimetric study demonstrates that both HT and VMAT achieve satisfactory HC sparing in WBRT while maintaining adequate target coverage and plan quality. Although PTV coverage, CI, and HI are comparable, VMAT offer shorter beam on time and better protection of critical organs particularly the eyes and HC by delivering lower maximum doses. VMAT may offer a more efficient and clinically advantageous approach for HCA-WBRT. These findings suggest that VMAT may be preferred for HCA-WBRT due to better OAR sparing and efficiency.

## Acknowledgments

### Statement of Transparency and Principles

- The authors declare no conflict of interest.
- The study was approved by the Research Ethics Committee of the authors' affiliated institution.
- The study data are available upon reasonable request.
- All authors contributed to the implementation of this research.

## References

1. Wen PY, Black PM, Loeffler JS. Metastatic brain cancer. In: DeVita V, Hellman S, Rosenberg SA, editors. *Cancer: Principles and Practice of Oncology*. 6th ed. Philadelphia: Lippincott Williams & Wilkins; 2001. p. 2655–2670...
2. Yang X, Ma L, Ye Z, Shi W, Zhang L, Wang J, Yang H. Radiation-induced bystander effects may contribute to radiation-induced cognitive impairment. *International Journal of Radiation Biology*. 2021;97(3):329-340. <https://doi.org/10.1080/09553002.2021.1864498>
3. Brown PD, Gondi V, Pugh S, Tome WA, Wefel JS, Armstrong TS, Bovi JA, et al. Hippocampal Avoidance During Whole-Brain Radiotherapy Plus Memantine for Patients With Brain Metastases: Phase III Trial NRG Oncology CC001. *Journal of Clinical Oncology: Official Journal of the American Society of Clinical Oncology*. 2020 04 01;38(10):1019-1029. <https://doi.org/10.1200/JCO.19.02767>
4. Gondi V, Hermann BP, Mehta MP, Tomé WA. Hippocampal dosimetry predicts neurocognitive function impairment after fractionated stereotactic radiotherapy for benign or low-grade adult brain tumors. *International Journal of Radiation Oncology, Biology, Physics*. 2012 07 15;83(4):e487-493. <https://doi.org/10.1016/j.ijrobp.2011.10.021>
5. Gondi V, Mehta MP, Pugh S, et al. Memory preservation with conformal avoidance of the hippocampus during whole-brain radiation therapy for patients with brain metastases: primary endpoint results of RTOG 0933. *Int J Radiat Oncol Biol Phys*. 2013;87(5):1186...
6. Raber J, Rola R, LeFevour A, Morhardt D, Curley J, Mizumatsu S, VandenBerg SR, Fike JR. Radiation-induced cognitive impairments are associated with changes in indicators of hippocampal neurogenesis. *Radiation Research*. 2004 07;162(1):39-47. <https://doi.org/10.1667/rr3206>
7. Tamura T, Sugihara G, Takahashi H. Memory Impairment and Hippocampal Volume after Carbon Monoxide Poisoning. *Archives of Clinical Neuropsychology: The Official Journal of the National Academy of Neuropsychologists*. 2021 01 15;36(1):145-148. <https://doi.org/10.1093/arclin/aaaa050>
8. Bremner JD, Hoffman M, Afzal N, Cheema FA, Novik O, Ashraf A, Brummer M, et al. The environment contributes more than genetics to smaller hippocampal volume in Posttraumatic Stress Disorder (PTSD). *Journal of Psychiatric Research*. 2021 05;137:579-588. <https://doi.org/10.1016/j.jpsychires.2020.10.042>
9. Toda T, Parylak SL, Linker SB, Gage FH. The role of adult hippocampal neurogenesis in brain health and disease. *Molecular Psychiatry*. 2019 01;24(1):67-87. <https://doi.org/10.1038/s41380-018-0036-2>
10. Lisman J, Buzsáki G, Eichenbaum H, Nadel L, Ranganath C, Redish AD. Viewpoints: how the hippocampus contributes to memory, navigation and cognition. *Nature Neuroscience*. 2017 Oct 26;20(11):1434-1447. <https://doi.org/10.1038/nn.4661>
11. Le Fèvre C, Cheng X, Loit M, Keller A, Cebula H, Antoni D, Thiery A, et al. Role of hippocampal location and radiation dose in glioblastoma patients with hippocampal atrophy. *Radiation Oncology*. 2021 06 22;16(1):112. <https://doi.org/10.1186/s13014-021-01835-0>
12. Gondi V, Tolakanahalli R, Mehta MP, Tewatia D, Rowley H, Kuo JS, Khuntia D, Tomé WA. Hippocampal-sparing whole-brain radiotherapy: a “how-to” technique using helical tomotherapy and linear accelerator-based intensity-modulated radiotherapy. *International Journal of Radiation Oncology, Biology, Physics*. 2010 Nov 15;78(4):1244-1252. <https://doi.org/10.1016/j.ijrobp.2010.01.039>
13. Eriksson PS, Perfilieva E, Björk-Eriksson T, Alborn AM, Nordborg C, Peterson DA, Gage FH. Neurogenesis in the adult human hippocampus. *Nature Medicine*. 1998 Nov;4(11):1313-1317. <https://doi.org/10.1038/3305>
14. Kuhn HG, Dickinson-Anson H, Gage FH. Neurogenesis in the dentate gyrus of the adult rat: age-related decrease of neuronal progenitor proliferation. *The Journal of Neuroscience: The Official Journal of the Society for Neuroscience*. 1996 03 15;16(6):2027-2033. <https://doi.org/10.1523/JNEUROSCI.16-06-02027.1996>
15. Monje ML, Mizumatsu S, Fike JR, Palmer TD. Irradiation induces neural precursor-cell dysfunction. *Nature Medicine*. 2002 09;8(9):955-962. <https://doi.org/10.1038/nm749>
16. Mizumatsu S, Monje ML, Morhardt DR, Rola R, Palmer TD, Fike JR. Extreme sensitivity of adult neurogenesis to low doses of X-irradiation. *Cancer Research*. 2003 07 15;63(14):4021-4027.
17. Glukhovskiy L, Brandstadter R, Leavitt VM, Krieger S, Buyukturkoglu K, Fabian M, Sand IK, et al. Hippocampal volume is more related to patient-reported memory than objective memory performance in early multiple sclerosis. *Multiple Sclerosis*. 2021 04;27(4):568-578. <https://doi.org/10.1177/1352458520922830>

18. Hubachek S, Botdorf M, Riggins T, Leong H, Klein DN, Dougherty LR. Hippocampal subregion volume in high-risk offspring is associated with increases in depressive symptoms across the transition to adolescence. *Journal of Affective Disorders*. 2021 02 15;281:358-366. <https://doi.org/10.1016/j.jad.2020.12.017>
19. Gondi V, Pugh SL, Tome WA, Caine C, Corn B, Kanner A, Rowley H, et al. Preservation of memory with conformal avoidance of the hippocampal neural stem-cell compartment during whole-brain radiotherapy for brain metastases (RTOG 0933): a phase II multi-institutional trial. *Journal of Clinical Oncology: Official Journal of the American Society of Clinical Oncology*. 2014 Dec 01;32(34):3810-3816. <https://doi.org/10.1200/JCO.2014.57.2909>
20. Kim J, Kim TG, Park B, Kim H, Song YG, Lee HW, Kim YZ, et al. Dosimetric comparison between RapidArc and HyperArc in hippocampal-sparing whole-brain radiotherapy with a simultaneous integrated boost. *Medical Dosimetry: Official Journal of the American Association of Medical Dosimetrists*. 2024;49(2):69-76. <https://doi.org/10.1016/j.meddos.2023.08.007>
21. Corrao G, Bergamaschi L, Eleonora Pierini V, Gaeta A, Volpe S, Pepa M, Zaffaroni M, et al. Hippocampal region avoidance in whole brain radiotherapy in brain metastases: For all or for some? A real-world feasibility report. *Tumori Journal*. 2024 02;110(1):34-43. <https://doi.org/10.1177/03008916231206926>
22. Liu R, Gong G, Meng K, Du S, Yin Y. Hippocampal sparing in whole-brain radiotherapy for brain metastases: controversy, technology and the future. *Frontiers in Oncology*. 2024;14:1342669. <https://doi.org/10.3389/fonc.2024.1342669>
23. Yokoyama K, Kurosaki H, Oyoshi H, Miura K, Utsumi N. Plan Quality Comparison Between Hippocampus-Sparing Whole-Brain Radiotherapy Treated With Halcyon and Tomotherapy Intensity-Modulated Radiotherapy. *Technology in Cancer Research & Treatment*. 2022;21:15330338221108529. <https://doi.org/10.1177/15330338221108529>
24. Jiang A, Sun W, Zhao F, Wu Z, Shang D, Yu Q, Wang S, et al. Dosimetric evaluation of four whole brain radiation therapy approaches with hippocampus and inner ear avoidance and simultaneous integrated boost for limited brain metastases. *Radiation Oncology*. 2019 03 15;14(1):46. <https://doi.org/10.1186/s13014-019-1255-7>
25. Andreas JJM, Kundapur V. Hippocampus Avoidance Whole-brain Radiation Therapy: A Practical Intensity-modulated Radiation Therapy Planning and Delivery Approach to RTOG 0933. *Journal of Medical Imaging and Radiation Sciences*. 2015 03;46(1):78-84. <https://doi.org/10.1016/j.jmir.2014.09.009>
26. Deepshikha G, Maji T, Lahiri D, Roy S, Bhanja S, Rangineni S, Ray DK, et al. Hippocampal avoidance whole brain radiotherapy in brain metastasis using volumetric modulated arc therapy: experience from a Regional Cancer Centre of Eastern India. *Reports of practical oncology and radiotherapy : journal of Greatpoland Cancer Center in Poznan and Polish Society of Radiation Oncology*. 2023 08 28;28(4). <https://doi.org/10.5603/RPOR.a2023.0048>
27. Li Z, Wang J, Deng L, Zhai Y, Zhang T, Bi N, Wang J, et al. Hippocampal avoidance whole-brain radiotherapy with simultaneous integrated boost in lung cancer brain metastases and utility of the Hopkins verbal learning test for testing cognitive impairment in Chinese patients: a prospective phase II study. *BMC cancer*. 2024 07 26;24(1):899. <https://doi.org/10.1186/s12885-024-12559-1>
28. Monje ML, Toda H, Palmer TD. Inflammatory blockade restores adult hippocampal neurogenesis. *Science*. 2003 Dec 05;302(5651):1760-1765. <https://doi.org/10.1126/science.1088417>
29. Bedford JL, Thomas MDR, Smyth G. Beam modeling and VMAT performance with the Agility 160-leaf multileaf collimator. *Journal of Applied Clinical Medical Physics*. 2013 05 06;14(2):4136. <https://doi.org/10.1120/jacmp.v14i2.4136>
30. Bae SH, Cho KH, Jung JH, Kim YS, Kim SG, Yoo J, Lee JM, et al. Stereotactic body radiotherapy using helical tomotherapy for hepatocellular carcinoma: clinical outcome and dosimetric comparison of Hi-ART vs. Radixact. *Translational Cancer Research*. 2022 Nov;11(11):3964-3973. <https://doi.org/10.21037/tcr-22-1565>



This work is licensed under a Creative Commons Attribution-Non Commercial 4.0 International License.